Supporting Information

Highly Bioactive Sol-Gel Derived Borate Glasses

William C Lepry and Showan N Nazhat*

Department of Mining and Materials Engineering, McGill University, Montreal, QC, Canada

*corresponding author showan.nazhat@mcgill.ca

Sol-Gel processing

A proposed process of gel formation is presented in Figure S1. It is thought that the hydrolysis and condensation reactions can both occur using the S_N mechanisms involving the nucleophilic attack of either the OR or OH ligands of the electrophilic, trigonal boron with the elimination of water or alcohol.[1]

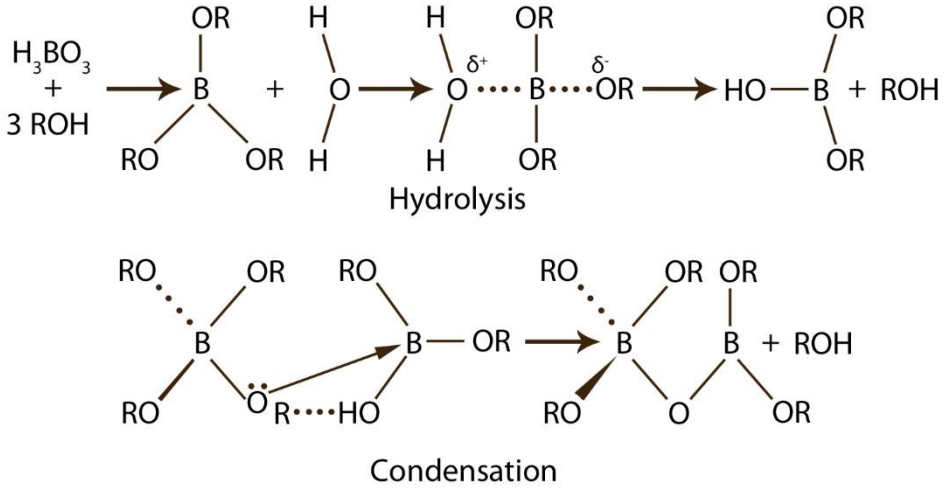

Figure S1. Gel network formation. A schematic showing the suggested route to borate glass network formation during the sol-gel process (recreated from Brinker *et al.* 1990)[1]

The ability of B36 in forming a gel monolith may have been impacted by its low borate (network forming oxide) content. Nevertheless, both of the formed phases were dried together and used for comparison purposes. Lower borate content gels appeared darker orange in colour (Figure S2a), and upon calcination, all glass particles appeared off-white (Figure 1). XRD

diffractograms of as-made glass particles displayed two broad humps indicating their amorphous and homogenous nature, except for B36, which displayed a number of minor peaks attributable to a precipitate phase (Figure S2b)

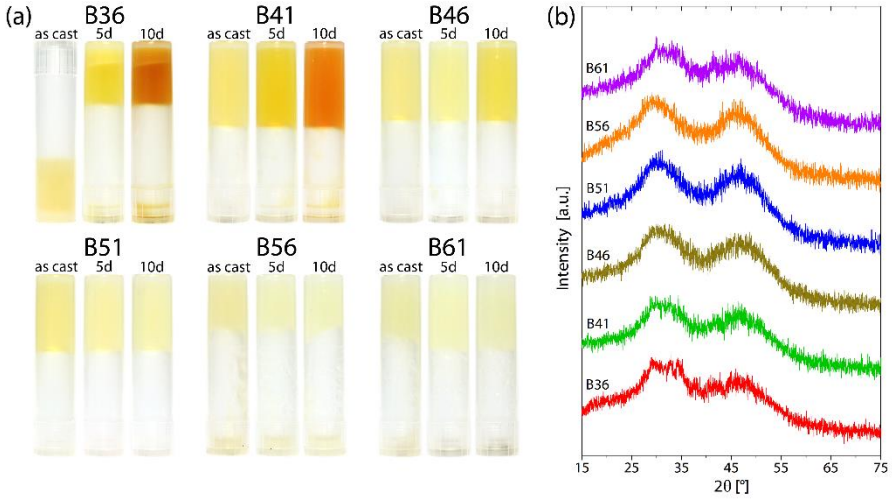

Figure S2. Sol-gel derived borate-based glasses. (a) Visual representation of the gels cast over the 10-day gelation period. B36 did not form a gel until day 3, where two distinct phases were observed. (b) XRD diffractograms of the as-made glasses displayed two broad humps indicating their amorphous nature. B36, on the other hand displayed a number of minor peaks, which may be due to a precipitated phase.

ATR-FTIR spectra of the as-made (AM) glasses displayed the peaks associated with borate-based glasses,[2-4] which were similar to and more defined than those of the calcined glasses (Figure S3). An increase in calcination temperature led to greater extents of crystallization as confirmed by the conversion of rounded peaks to more defined, sharp, doublet peaks. A calcination temperature of 400 °C ("Calcined") was chosen for the remainder of the study since all glasses remained amorphous at this temperature (Figure 2), which are likely to be more bioactive compared to partially crystallised glasses.[5]

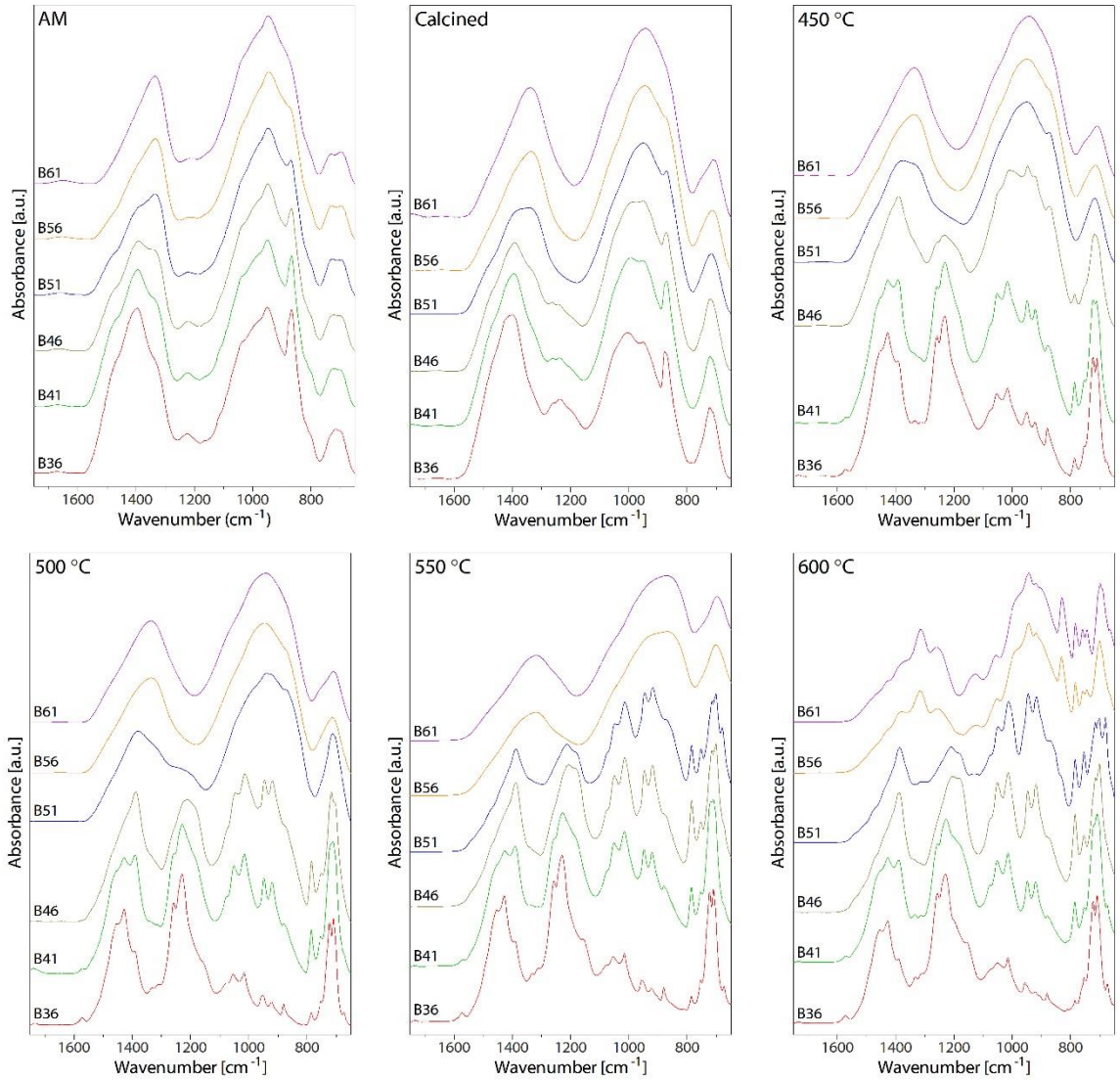

Figure S3. ATR-FTIR spectra of the SGBGs, as-made (AM) and calcined at different temperatures. Sharp, doublet peaks indicate increasing crystallization with calcination temperature, corroborating the XRD diffractograms shown in Figure 2.

Properties of calcined SGBGs

Reduction in glass surface area is the driving force in densification[6] and the SGBGs with lower borate content indicated the greatest extent of weight loss through calcination (Figure S4a). On the other hand, an increase in the calcination temperature of B46 led to a decrease in glass particle SSA and pore volume (Figure S4b).

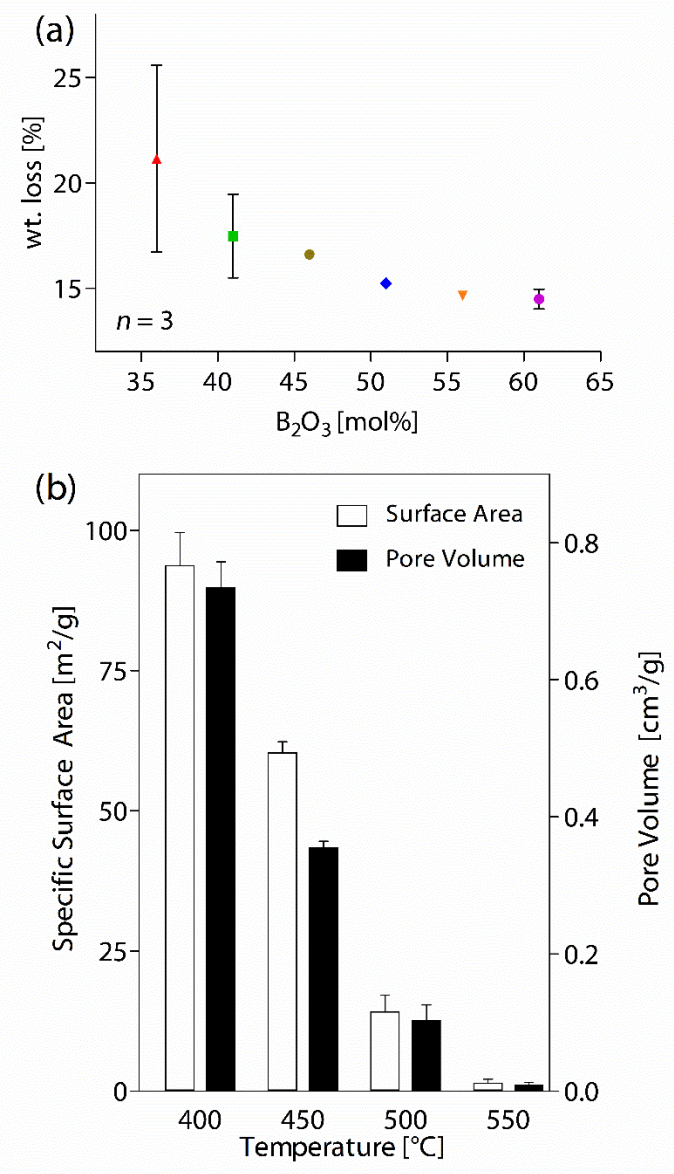

Figure S4. Properties of calcined SGBGs. (a) Percentage weight loss of SGBGs post calcination at 400 °C. Glasses with lower borate content experienced greatest extent of weight loss upon calcination. (b) Effect of calcination temperature on B46 SSA and pore volume. There was a decrease in these parameters with an increase in calcination temperature.

Calculation of SGBG network connectivity

Network connectivity (N_C), which has been used to predict the bioactivity of glasses,[7, 8] is a measure of the bridging oxygen bonds per network former (usually calculated for an Si atom in silicate-based glasses). N_C is measured on a scale of 0 to 4, with 4 indicating a fully connected,

chemically most stable network (e.g., quartz). On the other hand, glasses with an N_C between 2 and 2.6 have generally been regarded as bioactive,[9] *e.g.*, Bioglass® (45S5), which has an N_C of 2.12[7] as calculated using equation (1):

$$Nc = \frac{4(SiO_2) - 2[M_2^I O + M^{II} O] + 6[P_2 O_5]}{[SiO_2]} \quad (1)$$

where M^I and M^{II} represent glass network modifiers sodium and calcium, respectively. Modeling and NMR studies, have indicated that the phosphorous does not enter the glass network (*i.e.*, no Si – O – P bonds are formed) and remains as an orthophosphate [PO_4^{3-}], which is accounted for in the above calculation.[7] However, Si – O – P bonds can occur at higher P concentrations (> 50 mol%).[10]

In the case of borate-based glasses, while it is also possible to form B – O – P bonds,[11] as in the case of silicate-based glasses, it is assumed that the phosphorous does not enter the glass network and is present in an orthophosphate. In addition, if it is assumed that boron is 4-coordinted, as supported by the ATR-FTIR and NMR data (Figures 3a and b, respectively), then a similar N_C value can be calculated as that for Bioglass®. However, it should be noted that there are three main limitations to using this approach with sol-gel derived glasses, where: 1) the above calculation does not take into account the increased surface area and porosity; 2) not all boron is 4-coordinated; and 3) the sol-gel process results in residual OH^- groups on the surface, which may contribute to the bioactivity rates of the SGBGs in this study, even in N_C ranges where bioactivity is thought to be inhibited.[9] The latter, has been previously demonstrated for sol-gel derived silicate-based glasses.[12]

Measurement of DIW and SBF pH values in the presence of SGBGs

The extent of change in pH of the DIW and SBF solutions was dependent on SGBG composition (Figure S5), where lower borate content SGBGs resulted in higher pH values in both solutions, and can be attributed to higher extent of Na^+ ion release.[13]

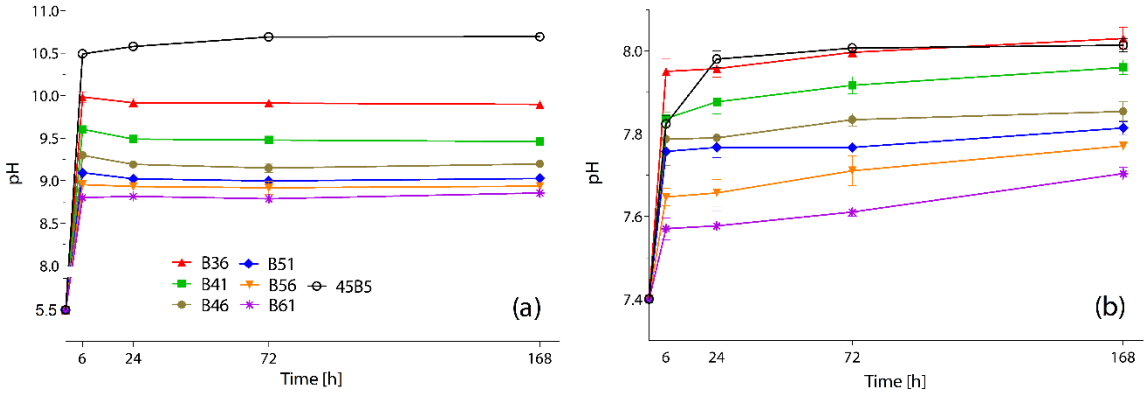

Figure S5. Effect of SGBG dissolution on the pH of (a) DIW and (b) SBF. The increase in pH values corresponded with SGBG composition, where glasses with lower borate content (*i.e.*, higher soda content) resulted in greater extents of pH increase.

SGBG mineralization in SBF

Figure S6 shows the SEM micrographs of all as-made and calcined (at 400 °C) SGBGs as a function of time in SBF. As-made and calcined SGBGs were comprised of textured porous surfaces, which became smoother after 6 h in SBF, attributable to the washing of loose nanoparticles. However, the surfaces regained their textured appearance with time in SBF, and by day 7, the typically observed HCA morphology was apparent, which correlated with XRD and ATR-FTIR (Figures 5 and 6, respectively).

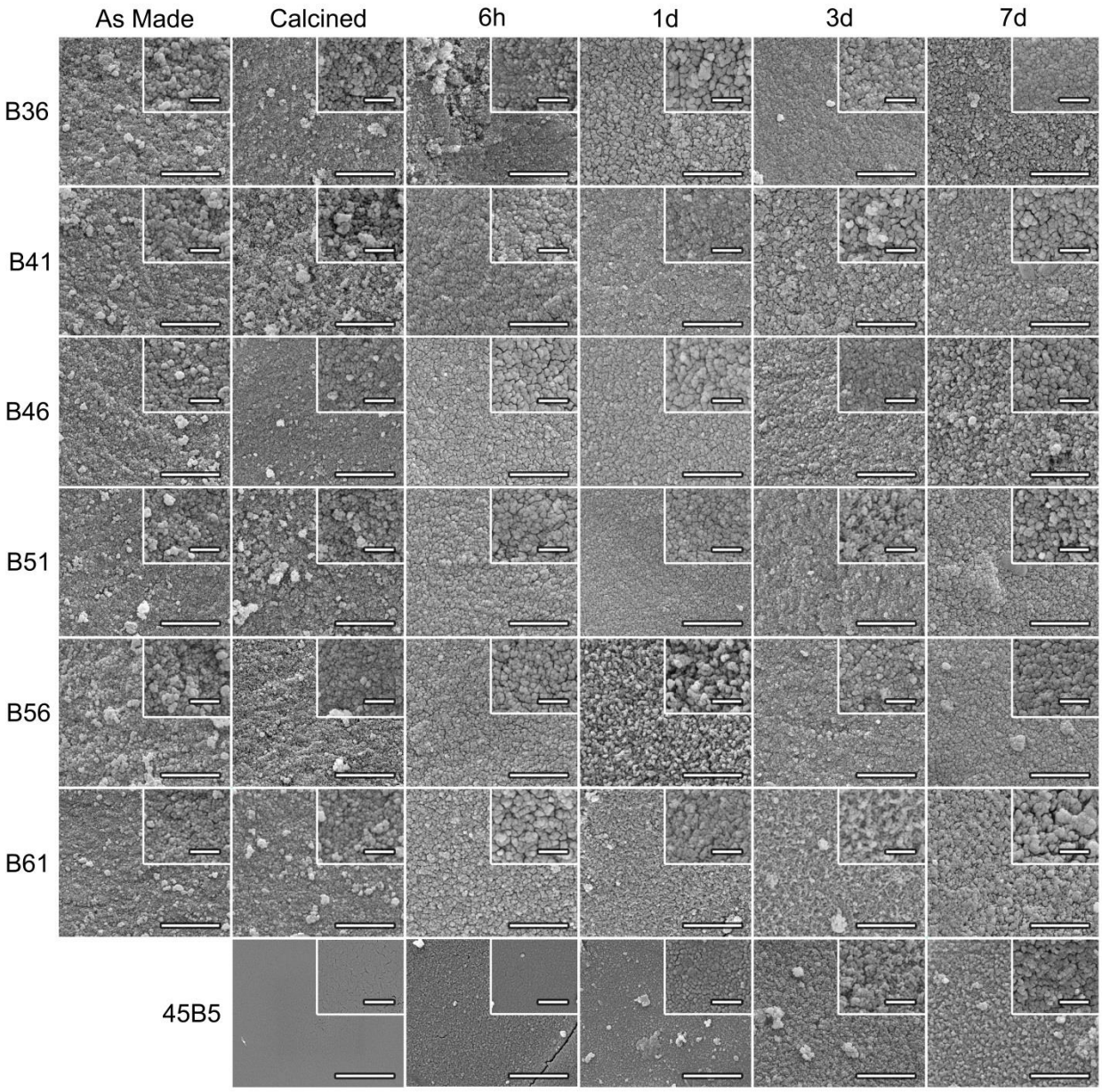

Figure S6. Morphology of SGBGs. SEM micrographs of all as-made and 400 °C calcined SGBGs as a function of time in SBF (scale bar = 2 μm, inset = 500 nm). Glass surfaces became more textured with time in SBF; attributable to HCA formation.

Comparing the mineralization of B46 and 45B5 in 0.02 M K_2HPO_4 solution

As a comparison to SBF, this study also investigated the mineralization of B46 and 45B5 in 0.02 M K_2HPO_4, which provided a 20 fold increase in phosphate content compared to SBF. It was found that apatite formation initiated within 6 h in both glasses, indicating that K_2HPO_4

artificially promotes rates of *in vitro* mineralization through the provision of excess, non-physiological concentrations of phosphate ions (Figure S7). Furthermore, the appearance of a sharper PO_4^{3-} peak and more pronounced shoulder regions in the ATR-FTIR spectra, indicated that the exposure to K_2HPO_4 did not favor the production of CO_3^{2-} and OH^- peaks, indicators of carbonated-apatite formation.

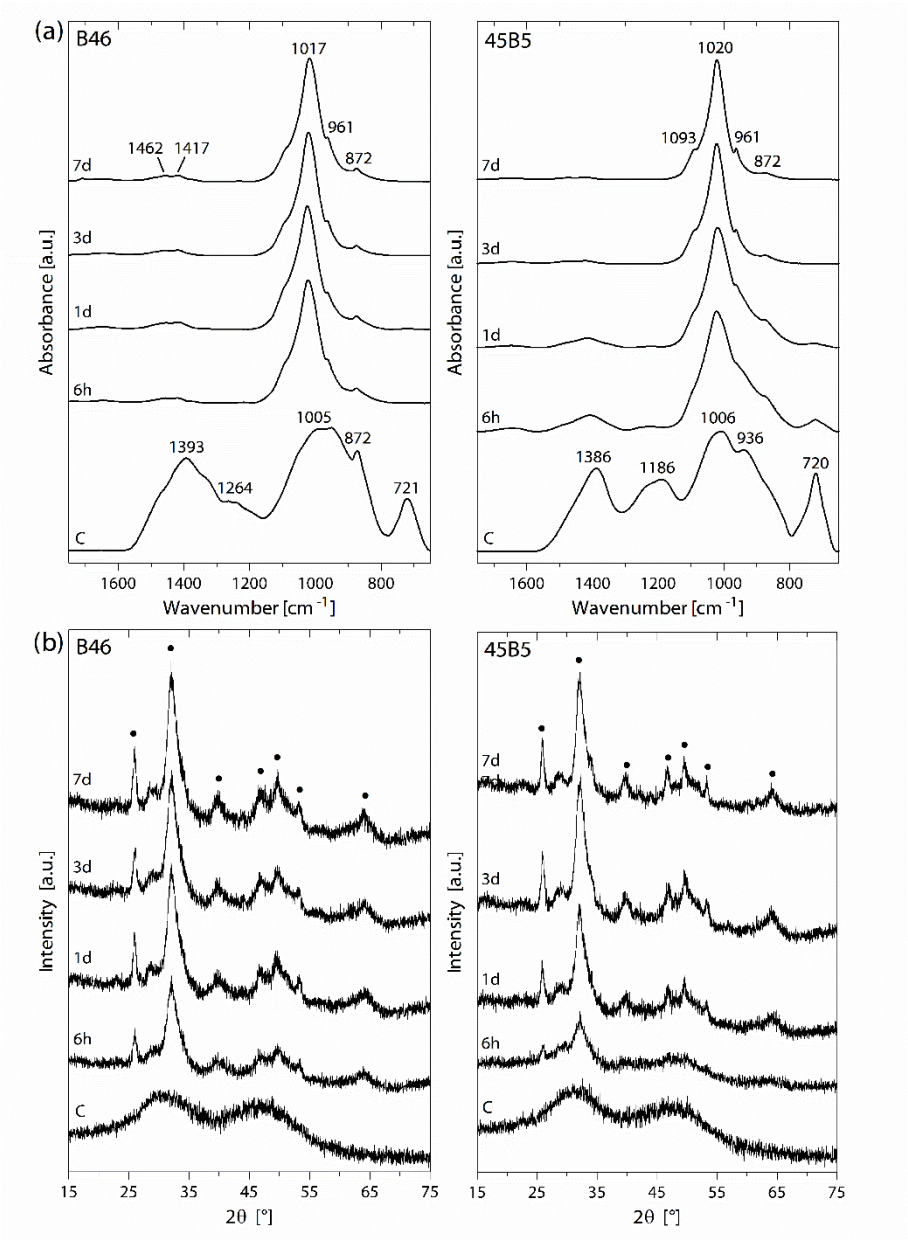

Figure S7. Mineralization rates of B46 and 45B5 in 0.02 M K_2HPO_4 solution. (a) ATR-FTIR spectra and (b) XRD diffractograms indicated that apatite peak formation initiated after 6 h in

both glasses demonstrating that the K_2HPO_4 solution is prone to giving favorable *in vitro* mineralization results.

SUPPLEMENTAL REFERENCES

1. Brinker, C. J.; Scherer, G. W. Sol-Gel Science: The Physics and Chemistry of Sol-Gel Processing. **1990**.
2. Kamitsos, E.; Karakassides, M.; Chryssikos, G. D. A vibrational study of lithium borate glasses with high Li_2O content. *Phys. Chem. Glasses* **1987,** *28*, 203-209.
3. Deliormanlı, A. M. In vitro assessment of degradation and bioactivity of robocast bioactive glass scaffolds in simulated body fluid. *Ceram. Inter.* **2012,** *38*, 6435-6444.
4. Kamitsos, E.; Karakassides, M.; Chryssikos, G. D. Vibrational spectra of magnesium-sodium-borate glasses. 2. Raman and mid-infrared investigation of the network structure. *J. Phys. Chem.* **1987,** *91*, 1073-1079.
5. Jones, J. R. Review of bioactive glass–from Hench to hybrids. *Acta Biomater.* **2012,** *9*, 4457–4486.
6. Whittemore Jr, O.; Sipe, J. Pore growth during the initial stages of sintering ceramics. *Powder Technol.* **1974,** *9*, 159-164.
7. Hill, R. G.; Brauer, D. S. Predicting the bioactivity of glasses using the network connectivity or split network models. *J. Non-Cryst. Solids* **2011,** *357*, 3884-3887.
8. Hill, R. An alternative view of the degradation of bioglass. *J. Mater. Sci. Lett.* **1996,** *15*, 1122-1125.
9. Edén, M. The split network analysis for exploring composition–structure correlations in multi-component glasses: I. Rationalizing bioactivity-composition trends of bioglasses. *J. Non-Cryst. Solids* **2011,** *357*, 1595-1602.
10. Li, A.; Wang, D.; Xiang, J.; Newport, R. J.; Reinholdt, M.; Mutin, P. H.; Vantelon, D.; Bonhomme, C.; Smith, M. E.; Laurencin, D. Insights into new calcium phosphosilicate xerogels using an advanced characterization methodology. *J. Non-Cryst. Solids* **2011,** *357*, 3548-3555.
11. Sharmin, N.; Hasan, M. S.; Parsons, A. J.; Furniss, D.; Scotchford, C. A.; Ahmed, I.; Rudd, C. D. Effect of boron addition on the thermal, degradation, and cytocompatibility properties of phosphate-based glasses. *BioMed Res. Int.* **2013,** 902427.
12. Li, R.; Clark, A.; Hench, L. An investigation of bioactive glass powders by sol-gel processing. *J. Appl. Biomater.* **1991,** *2*, 231-239.
13. Huang, W.; Day, D. E.; Kittiratanapiboon, K.; Rahaman, M. N. Kinetics and mechanisms of the conversion of silicate (45S5), borate, and borosilicate glasses to hydroxyapatite in dilute phosphate solutions. *J. Mater. Sci.: Mater. Med.* **2006,** *17*, 583-596.